A critical assessment of the elastic properties and effective wall thickness of single-walled carbon nanotubes

2008 Nanotechnology 19 075705

(http://iopscience.iop.org/0957-4484/19/7/075705)

Nanotechnology **19** (2008) 075705 (5pp) doi:10.1088/0957-4484/19/7/075705

A critical assessment of the elastic properties and effective wall thickness of single-walled carbon nanotubes

C Y Wang and L C Zhang[1]

The School of Aerospace, Mechanical and Mechatronic Engineering, University of Sydney, Sydney 2006, Australia

E-mail: L. Zhang@usyd.edu.au

Received 22 September 2007, in final form 15 December 2007
Published 31 January 2008
Online at stacks.iop.org/Nano/19/075705

Abstract

This paper discusses the fundamental issues of the elastic properties and effective wall thickness of single-walled carbon nanotubes (SWCNTs). It provides an in-depth analysis based on the rationale of the nanoscale-to-macroscale deformation relationship of SWCNTs and carries out a critical assessment of the diverse theoretical predictions in the literature. It was found that the in-plane stiffness of SWCNTs is a mechanics quantity that has been consistently reflected by the majority of the existing models. However, a further systematic study is necessary to clarify the dilemma of the wall thickness of SWCNTs.

1. Introduction

Carbon nanotubes (CNTs) [1] exhibit superior mechanical and electronic properties and hold substantial promise for structural/functional elements of nanocomposites [2] and nanoelectromechanical systems [3]. Most of these applications of CNTs depend crucially on their exceptional elastic properties; thus it is of central importance to accurately quantify the elastic properties of single-walled CNTs (SWCNTs). Particularly, if the effective thickness of SWCNTs can be well defined, the existing continuum models and numerical techniques developed for continuum bodies can be readily used for the characterization of CNTs and CNT-based nanostructures. Inspired by these motivations extensive studies [4–31] have been conducted to examine the above-mentioned issues in the past fifteen years. Unfortunately, considerable inconsistence has been found in the literature, where the values obtained for the same elastic stiffness are up to five times different [20, 24, 26] and the effective thickness of SWCNTs varies from 0.062 nm [20] to 0.69 nm [15]. To surmount these hurdles in describing macroscopic properties of SWCNTs, this paper aims to achieve an in-depth understanding of the causes of the inconsistent results in the literature and shed some lights on the long standing issue of the controversial effective thickness of SWCNTs. To characterize the macroscopic properties of SWCNTs, a SWCNT will be considered as an isotropic elastic thin shell of radius R, thickness h, Young's modulus E and Poisson ratio ν. The problem will then be investigated with other mechanics quantities, such as in-plane stiffness and off-plane stiffness, independent of the debatable values of E and h.

[1] Author to whom any correspondence should be addressed.

2. The in-plane stiffness K of SWCNTs

The in-plane stiffness K and bending stiffness D of a SWCNT modelled as an elastic shell are given as $K = \frac{Eh}{1-\nu^2} \approx Eh$ and $D = \frac{Eh^3}{12(1-\nu^2)} \approx \frac{Eh^3}{12}$ [32, 33], respectively. On the basis of these formulae, once K and D of a SWCNT are determined without knowing E and h they can be used to produce E and h to possibly clarify the inconsistence of E and h, and finally determine the two most fundamental mechanics quantities.

In this section let us first discuss the in-plane stiffness $K \approx Eh$ of SWCNTs. (It is noted that the equivalent modulus $E\beta$ discussed by Wang *et al* [34] is similar to the concept Eh, where β is the thickness-to-diameter ratio.) In most cases, a SWCNT under uniaxial force F_{axial} is considered in virtual experiments to measure its in-plane stiffness K or Young's modulus E. Specifically, without defining effective thickness of SWCNTs the K value can be directly calculated via the energy method, i.e., $K = \frac{1}{V_\alpha} \cdot \frac{\partial^2 W(\varepsilon_{\text{axial}})}{\partial \varepsilon_{\text{axial}}^2}$ [4–6, 8, 9, 12, 13, 16, 19, 23–26], or

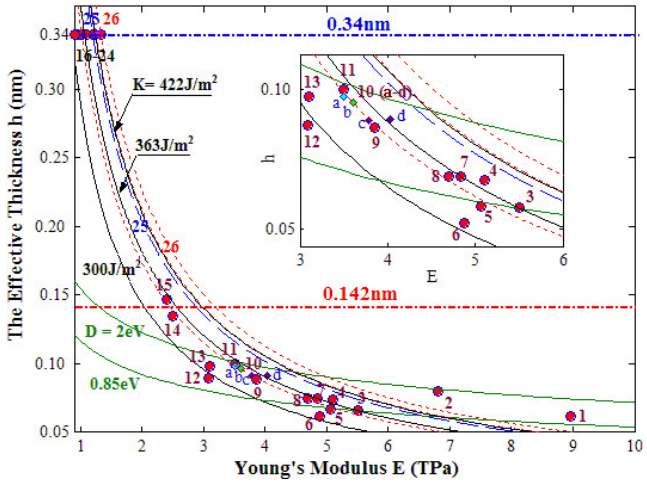

Figure 1. The effective thickness h, Young's modulus E, in-plane stiffness $K = \frac{Eh}{1-\nu^2} \approx Eh$ and the bending stiffness $D = \frac{Eh^3}{12(1-\nu^2)}$ obtained in the literature for SWCNTs, where ν is Poisson's ratio. Among the five solid lines two represent bending stiffness $D = \frac{Eh^3}{12(1-\nu^2)} \approx \frac{Eh^3}{12} = 0.85$ eV and 2 eV, respectively. The other three solid lines are associated with increasing in-plane stiffness $K = \frac{Eh}{1-\nu^2} \approx Eh = 300$, 360 and 422 J m^{-2}. Dots 10(a–d) are given by [9]. The models and sources of the dots in the figure are listed in table 1.

(This figure is in colour only in the electronic version)

the force method, i.e., $K = \frac{F_{\text{axial}}/\varepsilon_{\text{axial}}}{2\pi R}$ [13, 14, 18, 22, 24], where V_α is the volume of a carbon atom, $\varepsilon_{\text{axial}}$ is axial strain and $W(\varepsilon_{\text{axial}})$ is the strain energy shared by each carbon atom in SWCNTs. Various techniques, e.g., *ab initio* (dots 5, 9, 10 in figure 1) [9, 13, 27], local density approach (dot 8) [16], tight-binding (TB) model (dots 4, 20, 22) [6, 10, 12], molecular dynamics (MD) simulations (dots 2, 3, 16, 17, 20, 22, 24) [4, 5, 8, 14, 19, 22, 28], force constant model (dot 17) [25], structural mechanics (SM) model (dot 19) [18], molecular mechanics (MM) model (dots 13, 14) [24] and finite element method (FEM) (dot 15) [26], have been used to calculate $\varepsilon_{\text{axial}}$ or $W(\varepsilon_{\text{axial}})$ in virtual experiments and finally determine K via aforementioned formula. Here the SM, MM and MD simulations as well as FEM are based on different empirical potentials, such as the Tersoff–Brenner potential [4, 14, 22, 24], universal force field potential [5], molecular mechanics 3 (MM3) potential [24], modified Mores potential [14], and harmonic potential [18, 19, 26]. Alternatively the K value can also be extracted via the continuum–atomistic model fitting in studying phonon dispersion relation (dot 11) of SWCNTs [31]. In addition to these, the values of K associated with (dots 6) [20] is estimated via $K = \frac{Eh}{1-\nu^2} \approx Eh$ based on the values of E and h obtained in a ring–atomistic model fitting for radial pressure–induced bending of SWCNTs and those corresponding to dots 1 and 12 [17] are obtained (for armchair and zigzag tubes, respectively) based on a continuum model of atomic bond (CMAB), where σ bond stretching and bond angle bending are modelled simply with stretching and rotating springs.

As shown in figure 1, the majority of the previous results (dots 1–24) are dispersed in the vicinity of the curve corresponding to $K \approx Eh = 360$ J m^{-2}, with the lowest K around 300 J m^{-2} (dot 6) and the highest around 420 J m^{-2} (dots 23 and 24). This shows that different modelling techniques are generally in reasonable agreement in predicting in-plane stiffness of SWCNTs. Thus, in figure 1 the wide scatter of Young's modulus varying from 0.9 TPa (dot 15) to 9 TPa (dot 1), are essentially a result of different choices of the effective thickness of SWCNTs. Here, the consistency of the in-plane stiffness suggests that the in-plane deformation of SWCNTs interpreted solely as a result of σ bond stretching and angle bending can be adequately described by almost all aforementioned atomistic theories. Indeed, as shown in [19] and [24], different calculation methods, i.e., the energy and force methods, and various empirical potentials used in MM/SM/MD simulations, e.g., the Tersoff–Brenner potential, modified Mores potential, MM3 potential, and harmonic potential, only result in relatively small variation (6–11%) of the value of Young's modulus (with the same value of the effective thickness) or equivalent in-plane stiffness K.

Experimentally 'measured' Young's modulus of long SWCNTs is also presented in figure 1, where the equivalent in-plane stiffness K is obtained by fitting the Euler beam model to the data measured in thermal vibration (a dashed line labelled 25) [7], or by three-point bending experiments (three dotted lines labelled 26 (for three samples) [11]). It is seen that the values of the in-plane stiffness given by the two experiments are generally consistent with the theoretical results and therefore, can be viewed as a validation that the theoretically predicted K value of SWCNTs is correct, which is around 360 J m^{-2}.

On the other hand, there are a few exceptions, as also shown in figure 1. Three results, i.e., dot 2 from [28] and dots 1 and 12 given by [17] for armchair and zigzag tubes, respectively, are away from the zone of all other theoretical and experimental results. As stated in [28], the discrepancy between this work [28] and other theoretical studies arises from the different range of axial strain considered in the virtual tensile experiment, i.e., while others considered axial tension within a very small strain level (e.g., smaller than 1%), reference [28] investigated the larger strain regime up to 5% because the authors [28] observed that SWCNTs display linear elastic characters only at a relatively large strain, e.g., 5%. However, according to Mylvaganam and Zhang [35], within the strain range of up to 5% for armchair SWCNTs and 8% for zigzag SWCNTs, the mechanical behaviour of a SWCNT does not change dramatically. Thus this argument for the higher value of in-plane stiffness reported in [28] cannot be justified straightforwardly, and needs to be further investigated. Additionally, in [17] the K value of armchair SWCNTs is 554 J m^{-2} (dot 1) which is twice as much as 277 J m^{-2} (dot 12) reported for zigzag tubes. The result is however inconsistent with almost all other studies [5, 6, 8, 18, 19, 27, 36, 37], where it is shown that the chirality of SWCNTs with radius larger than 1 nm has negligible effect on their elastic properties. Thus the rationale of the derivation or the validity of the model used in [17] need to be further examined.

3. The bending stiffness D of SWCNTs

In figure 1, the bending stiffness D of SWCNTs given by dots 3, 4, 5, 9 and 10(a–d) (see inset of figure 1) are calculated by using $D = \frac{1}{V_a} \cdot \frac{\partial^2 W(\kappa)}{\partial \kappa^2}$ [4, 9, 12, 13, 27], where $W(\kappa)$ represents the energy (i.e., rolling energy) that is required to roll up a flat graphite sheet to a cylindrical surface and κ denotes the curvature change in this process. Here the values of $W(\kappa)$ from different sources were calculated by using MD simulation (dot 3) [4], TB model (dot 4) [12], *ab initio* calculation (dots 5, 9, 10) [9, 13, 27] or FEM (dot 7) [23]. Another way to extract the D value of SWCNTs is to fit elastic shell models to atomistic models in predicting strain energy (dots 8) [16] or phonon dispersion relation (dot 11) [31] of SWCNTs or calculate the D value (dots 1 and 12 for armchair and zigzag SWCNTs [17]) based on an existing MM model for dihedral inversion of SWCNTs [38]. In addition, the D values associated with dots 2, 6, 13, 14 and 15 are estimated via $D = \frac{Eh^3}{12(1-\nu^2)} \approx \frac{Eh^3}{12}$ based on the values of E and h obtained in [20, 24, 26, 28].

Figure 1 shows that the D values of SWCNTs reported in the literature locate in the following different regimes, i.e., 0.69–0.85 eV (dots 3, 5, 6), 1–1.3 eV (dots 1, 4, 7, 8, 12), 1.49–2 eV (dots 2, 9–11, 13), and 3.28 eV or larger (dots 14–15). The cause of the diversity of the D values can be related to the unclear links between the continuum mechanics approach and the atomistic structure of an SWCNT. For example, the LDA [16] (dot 8) shows that both the σ bond changes, and the π electron resonance, especially the π orbital electron density change due to the dihedral inversion of graphitic plane, contribute to the bending resistance of a SWCNT. This theory is also used in [23] to explain the origin of the bending stiffness of a SWCNT. Nevertheless, the MM model [15, 38, 39] for the bending of SWCNTs used in [17] (dots 1 and 12) assumes that the D value of a SWCNT is merely determined by the change of the π orbital electron density due to the dihedral inversion. In the meantime, as shown in [21] and [40] the Tersoff–Brenner potential [41–43] adopted in [4] (dot 3) indicates that only the change of σ bond is responsible for the bending resistance of a SWCNT. Furthermore, we can see in [44] that little agreement has been reached in modelling the atomic bond inversion of dihedral structures, for which five different models have been suggested, i.e., AMBER, CHARMM, GROMOS, the Tripos 5.2 and the DREIDING [44]. Similarly, in studying the relation between D and σ bond changes, [21] shows that D depends on both σ bond stretching and angle bending, and [16, 23, 40] demonstrate that only the angle bending is related to D. Here, it is worth mentioning that by looking into [21, 24, 40], the Tersoff–Brenner potential [41–43] widely used in MM/MD simulations of CNTs can capture the length and angle changes of the σ bond but cannot fully accounts for the effect of the π orbital on the off-plane deformations of SWCNTs. This in fact explains why the Tersoff–Brenner potential [41–43] leads to the π orbital-independent bending stiffness D [21, 40] and unintuitive zero off-plane torsion stiffness [40], which, as shown in [16, 29], is determined only by the π electron resonance with its value around 0.8 eV [16, 29, 31]. On the other hand, in [21, 40] the Tersoff–Brenner potential [41–43] gives the bending stiffness of SWCNTs as a function of the first derivative of the inter-atomic potential with respect to σ bond length r_{ij} (between atoms i and j with equilibrium bond length r_0) and/or angle θ_{ijk} (between the bonds i–j and i–k with equilibrium bond angle θ_0). This reveals that choosing the harmonic potential U, i.e., $U \propto A \cdot \sum_{\text{length}} (r_{ij} - r_0)^2 + B \cdot \sum_{\text{angle}} (\theta_{ijk} - \theta_0)^2$ for σ bond stretching and angle bending will automatically lose the σ bond contribution to the bending stiffness of SWCNTs. Thus the FEM [26], MM models [36, 37] and MD simulations [19, 28] based on the harmonic potential cannot give accurate description to the mechanical behaviour of SWCNTs sensitive to the bending stiffness D. In view of all these, more accurate atomistic models that are capable of accurately estimating the contributions from both the σ bond and the π bond are necessary to give consistent depiction of the bending stiffness of SWCNTs. Meanwhile, well-controlled nanoscale experiments are essential to validate the accuracy and applicability of the theoretical methods.

As mentioned before the D values in figure 1 associated with dots 2, 6, 13, 14 and 15 are estimated via the classic shell formula $D = \frac{Eh^3}{12(1-\nu^2)} \approx \frac{Eh^3}{12}$, where the values of E and h are extracted by fitting different continuum models to atomistic simulations. It is seen that when a shell (tube) model [24, 28] is used in calculating E and h the corresponding D values (dots 2 and 13) are close to those given by TB model (dot 4) [12], LDA (dot 8) [16], and *ab initio* calculation (dots 5, 9 and 10) [9, 13, 27]. In contrast, the E and h values obtained for a ring model [20] or a structure frame model [26] make the D values (dots 6 or 15) significantly smaller or larger than those calculated directly based on atomistic simulations at dots 4–5 and 9–10. These suggest that if the D value is calculated based on $D = \frac{Eh^3}{12(1-\nu^2)} \approx \frac{Eh^3}{12}$ for an equivalent shell the different continuum models used in extracting E and h values could also contribute to the scatter of the D value. For example, the effective thickness of 0.147 nm [26] given by dot 15 is in fact the diameter of the microbeams used to describe inter-atomic interaction between two adjacent atoms, which, as will be shown later, is obviously larger than the effective thickness of an equivalent shell of a SWCNT and thus leads to the D value much higher than all the results obtained by other means. In addition, the significantly different D values (100% different) of dots 13 and 14 [24] are caused by the two different potentials used in calculation, i.e., the Tersoff–Brenner potential and MM3 potential (see table 1). This shows that the bending stiffness D is much more sensitive to the potential than the in-plane stiffness K (note dots 13 and 14 give the K values which are close to each other).

The role of Poisson's ratio ν of SWCNTs to the in-plane stiffness K and bending stiffness D is to couple between the axial and circumferential deformations, i.e., $\nu = -\varepsilon_\theta/\varepsilon_x$, where ε_x and ε_θ denote normal axial and circumferential strains, respectively, in uniaxial tension/compression. In the literature, the ν values given by *ab initio* [9, 13, 27], TB mode [6], MD/MM simulations [4, 24] and force constant model [5], range from 0.144 to 0.28, which is not very different from that of graphite (0.16) used in [25]. The noticeable radius and chirality dependence of ν is observed for fine SWCNTs with diameter not larger than 1 nm [9, 27]. In addition, higher

Table 1. Models and references corresponding to the dots in figure 1. (Note: CMAB: continuum model of atomic bond; SM: structural mechanics; TB: tight-binding; LDA: local density approach; MM: molecular mechanics; FEM: finite element method; MD: molecular dynamics; FC: force constant; UFF: universal force field; T–B potential: Tersoff–Brenner potential; M-M potential: modified Morse potential.)

Dot	Model	Reference	Dot	Model	Reference
1	CMAB	[17]	14	MM model (MM3 potential)	[24]
2	MD simulation (*ab initio* force field potential)	[28]	15	FEM	[26]
3	MD simulation (T–B potential)	[4]	16	MD simulation (T–B potential)	[22]
4	TB model	[12]	17	FC model	[25]
5	*ab initio*	[27]	18	MD simulation (UFF potential)	[5]
6	Ring model	[20]	19	SM simulation (harmonic potential)	[18]
7	Shell model	[23]	20	MD simulation (UFF potential)	[8]
8	LDA model	[16]	21	TB model	[10]
9	*ab initio*	[13]	22	MD simulation (M-M potential)	[14]
10	*a*[a] *b* tube (10, 0) *c* tube (8, 4) *ab initio* *d* tube (*n*, *n*)	[9]	23	TB model	[6]
11	Shell–lattice fitting	[31]	24	MD simulation (harmonic potential)	[19]
12	CMAB	[17]	25	Thermal vibration	[7]
13	MM model (T–B potential)	[24]	26	3-point bending	[11]

[a] The values of elastic constants are estimated from the quadratic behaviour of the ZA band in the phonon dispersion relation of SWCNTs.

ν values, i.e., 0.34 [16] and 0.4 [27], are also obtained based on the LAD [16] and FEM [27], respectively. It is easy to understand that Poisson's ratio only plays a minor role in determining the effective thickness h and Young's modulus E of SWCNTs, simply because in the shell formulae, i.e., $K = \frac{1}{1-\nu^2} \cdot (Eh)$ and $D = \frac{1}{1-\nu^2} \cdot (\frac{Eh^3}{12})$, the coefficient $\frac{1}{1-\nu^2}$ only varies from 1.02 to 1.16, when ν varies from its minimum, 0.144, to its maximum, 0.4.

4. The effective thickness *h*

By plotting the values of the effective thickness of SWCNTs together in a single diagram, as in figure 1, we can see that they fall into two large groups; One is the assumed value of 0.34 nm (dots 16–24) [5–8, 10, 11, 14, 18, 19, 22, 25], which is the interlayer spacing of multi-walled CNTs, and the other is a group of values derived based on different theoretical methods (dots 1–15) [4, 9, 12, 13, 16, 17, 20, 23, 24, 27, 28, 31]. Among the totally fifteen theoretical predictions, fourteen fall in the range between 0.0617 nm [20] and 0.134 nm [24], and thus, satisfy the Vodenitcharova–Zhang criterion [20] that the effective wall thickness of SWCNTs must be smaller than the atomic diameter of carbon atoms, 0.142 nm. So far, only two exceptions have been found; i.e., 0.69 nm [15] (not shown in figure 1) and 0.147 nm [26]. These results show that the Vodenitcharova–Zhang criterion [20] can indeed be used as a guideline for future research work on the effective thickness of SWCNTs. For details of this criterion the reader may refer to [20].

It should be pointed out that the previously proposed effective thickness of 0.34 nm is not applicable due to the following reasons. First this value was proposed as an assumption instead of being derived based on any physical understanding. Specifically, as shown in figure 1, this effective thickness and the corresponding Young's modulus lead to an extremely high bending stiffness of SWCNTs, an order of magnitude higher than all the theoretical predictions (experimental measurement is not available). Also, it is obvious that the value of 0.34 nm violates the Vodenitcharova–Zhang criterion. Similarly, the values of 0.69 nm and 0.147 nm which cannot satisfy the Vodenitcharova–Zhang criterion should also be excluded in future discussion. Particularly, $h = 0.69$ nm [15] (not shown in figure 1) results in even worse bending stiffness of SWCNTs as compared with the value of 0.34 nm. In addition, as mentioned in section 2, $h = 0.147$ nm obtained by [26] is the effective diameter of equivalent microbeams used in structure frame model [26] to describe the inter-atomic action in SWCNTs. Following the physical understanding of Vodenitcharova and Zhang [20] this value is obviously too large, violating the basic force equilibrium requirement.

As shown in [16, 29–31], to obtain a well-defined effective thickness for a SWCNT modelled as an isotropic shell the elastic stiffness of the SWCNT must satisfy the condition $\frac{D}{K} = \frac{D_{\text{torsion}}}{K_{\text{torsion}}}$ [32, 33] where D_{torsion} and K_{torsion} are off-plane

and in-plane torsion stiffnesses, respectively. However, while this condition is found to be true in [16, 31] for SWCNTs, the analysis based on a recent LDA model gives a negative answer [29, 30] making the authors of [29, 30] conclude that a three-dimensional isotropic shell with well-defined thickness does not exist for SWCNTs. Indeed, since the bending deformation mechanism of a SWCNT as a three-dimensional discrete structure is quite different from that of an elastic shell (see details in [32, 33]), $\frac{D}{K} = \frac{D_{\text{torsion}}}{K_{\text{torsion}}}$, which is satisfied by any isotropic continuum shell, may not be reached by their counterparts of SWCNTs. If this conclusion can finally be confirmed by accurate atomistic simulations, an anisotropic shell model, e.g., an orthotropic shell may be developed to define effective thickness for SWCNTs without satisfying the aforementioned condition derived for isotropic shells.

5. Conclusions

On the basis of the above critical assessment we can observe the following:

(1) Atomistic models consistently show that the in-plane deformation of SWCNTs is controlled by the bond length and angle change of in-plane σ bond. The mostly agreed value of in-plane stiffness K by different atomistic models is around 360 J m^{-2}.

(2) The bending deformation of SWCNTs is governed by both the change of in-plane σ bond and inversion of off-plane π orbital. The large scatter of the value of bending stiffness reported in the literature can be partially attributed to the fact that different atomistic models are inconsistent in modelling the bending deformation or evaluating the contributions from the two atomic bonds to bending resistance of SWCNTs. Thus, to resolve this problem more accurate atomistic model validated by accurately controlled nanoexperiments is needed.

(3) The Tersoff–Brenner potential, widely used for MM/MD simulation of CNTs cannot accurately account for the π orbital contribution to the off-plane deformations of SWCNTs, e.g., bending and off-plane torsion, and therefore cannot give accurate value of the bending stiffness and off-plane torsion stiffness for SWCNTs.

(4) The Vodenitcharova–Zhang criterion that the effective thickness of SWCNTs should be smaller than the atomic diameter 0.142 nm should be used as a necessary condition (but not sufficient) for justifying an effective thickness of SWCNTs. The assumed value of 0.34 nm as well as those larger than 0.142 nm, e.g., 0.69 and 0.147 nm should be excluded in future investigations.

Acknowledgment

This work was supported by an ARC Discovery Grant.

References

[1] Iijima S 1991 *Nature* **354** 56
[2] Qian D, Wagner G J, Liu W K, Yu M F and Ruoff R S 2002 *Appl. Mech. Rev.* **55** 495
[3] Baughman R H, Zakhidov A A and de Heer W A 2002 *Science* **297** 787
[4] Yakobson B I, Brabec C J and Bernholc J 1996 *Phys. Rev. Lett.* **76** 2511
[5] Lu J P 1997 *Phys. Rev. Lett.* **79** 1297
[6] Hernández E, Goze C, Bernier P and Rubio A 1998 *Phys. Rev. Lett.* **80** 4502
[7] Krishnan A, Dujardin E and Ebbesen T W 1998 *Phys. Rev.* B **58** 14013
[8] Yao N and Lordi V 1998 *J. Appl. Phys.* **84** 1939
[9] Sanchez-Portal D, Artacho E and Soler J M 1999 *Phys. Rev.* B **59** 12678
[10] Ozaki T, Iwasa Y and Mitani T 2000 *Phys. Rev. Lett.* **84** 1712
[11] Tombler T W, Zhou C W, Alexseyev L, Kong J, Dai H J, Liu L, Jayanthi C S, Tang M J and Wu S Y 2000 *Nature* **405** 769
[12] Zhou X, Zhou J and Zhong-Can O Y 2000 *Phys. Rev.* B **62** 13692
[13] Kudin K N, Scuseria G E and Yakobson B I 2001 *Phys. Rev.* B **64** 235406
[14] Belytschko T, Xiao S P, Schatz G C and Rouft R S 2002 *Phys. Rev.* B **65** 235430
[15] Odegard G M, Gates T S, Nicholson L M and Wise K E 2002 *Compos. Sci. Technol.* **62** 1869
[16] Tu Z C and Ou-Yang Z C 2002 *Phys. Rev.* B **65** 233407
[17] Wang Q 2002 *Int. J. Solids Struct.* **39** 3893
[18] Li C and Chou T W 2003 *Int. J. Solids Struct.* **40** 2487
[19] Jin Y and Yuan F G 2003 *Compos. Sci. Technol.* **63** 1057
[20] Vodenitcharova T and Zhang L C 2003 *Phys. Rev.* B **68** 165401
[21] Arroyo M and Belytschko T 2004 *Phys. Rev.* B **69** 115415
[22] Bao W X, Zhu C C and Cui W Z 2004 *Physica* B **352** 156
[23] Pantano A, Parks D M and Boyce M C 2004 *J. Mech. Phys. Solids* **52** 789
[24] Sears A and Batra A C 2004 *Phys. Rev.* B **69** 235406
[25] Shen L X and Li J 2005 *Phys. Rev.* B **71** 165427
[26] Tserpes K I and Papanikos P 2005 *Composites* B **36** 468
[27] Wang L F, Zheng Q S, Liu J Z and Jiang Q 2005 *Phys. Rev. Lett.* **95** 105501
[28] Chen X and Cao G 2006 *Nanotechnology* **17** 1004
[29] Tu Z C and Ou-Yang Z C 2006 *J. Comput. Theor. Nanosci.* **3** 375
[30] Tu Z C and Ou-Yang Z C 2007 *J. Comput. Theor. Nanosci.* at press
[31] Wang C Y and Zhang L C 2007 *Nanotechnology* submitted
[32] Timoshenko S 1940 *Theory of Plates and Shells* (New York: McGraw-Hill)
[33] Flugge W 1973 *Stress in Shells* 2nd edn (Berlin: Springer)
[34] Wang M, Qiu X M, Zhang X and Yin Y J 2007 *Nanotechnology* **18** 295708
[35] Mylvaganam K and Zhang L C 2004 *Carbon* **42** 2025
[36] Chang T C and Gao H J 2003 *J. Mech. Phys. Solids* **51** 1059
[37] Shen L X and Li J 2004 *Phys. Rev.* B **69** 045414
[38] Bakowies D and Thiel W 1991 *J. Am. Chem. Soc.* **113** 3704
[39] Adams G, Sankey O, Page J, O'Keeffe M and Drabold D 1992 *Science* **256** 1792
[40] Huang Y, Wu J and Hwang K C 2006 *Phys. Rev.* B **74** 245413
[41] Tersoff J 1988 *Phys. Rev.* B **37** 6991
[42] Brenner D W 1990 *Phys. Rev.* B **42** 9458
[43] Brenner D W, Shenderova O A, Harrison J A, Stuart S J, Ni B and Sinnott S B 2002 *J. Phys.: Condens. Matter* **14** 783
[44] Rappe A K and Casewit C J 1997 *Molecular Mechanics Across Chemistry* (Mill Valley, CA: University Science Books)